Organic & Biomolecular Chemistry

Dynamic Article Links

Cite this: *Org. Biomol. Chem.*, 2011, **9**, 8261

www.rsc.org/obc

PAPER

4′-Alkoxy oligodeoxynucleotides: a novel class of RNA mimics†

Radek Liboska,[a] Jan Snášel,[a] Ivan Barvík,[b] Miloš Buděšínský,[a] Radek Pohl,[a] Zdeněk Točík,[a] Ondřej Páv,[a] Dominik Rejman,[a] Pavel Novák[a] and Ivan Rosenberg*[a]

Received 12th July 2011, Accepted 2nd September 2011
DOI: 10.1039/c1ob06148h

4′-Alkoxy-oligothymidylates were prepared as model compounds to study the influence of a C4′-alkoxy group on hybridisation. The phosphodiester homooligomers (15 units long) containing either a 4′-methoxy or 4′-(2-methoxyethoxy) group were found to display increased hybridisation with both dA_{15} and rA_{15} complementary counterparts compared to the natural oligothymidylate. In addition, we found their hybridisation behaviour to be similar to that of the regioisomeric 2′-*O*-methyl-oligothymidylate. The formed complexes (duplexes and triplexes) were studied using UV spectroscopy and polyacrylamide gel electrophoresis (PAGE). Structural background of the hybridization behaviour was examined using NMR and MDS. The favourable hybridisation properties of the 4′-alkoxyoligothymidylates indicated that 4′-alkoxy modified nucleotides are promising compounds for the assembly of chimeric oligonucleotides with tunable properties.

Introduction

Attempts to use synthetic oligonucleotides (ONs) as tools for the regulation of gene expression, starting with the original antisense concept by Zamecnik,[1] has necessitated diverse chemical modifications of the natural oligomeric chains to improve their hybridisation capabilities, resistance toward nucleases, uptake into cells, and RNase H activation to convert them into therapeutic candidates.[2–5] After exploitation of phosphorothioates[6] as the first-generation of antisense compounds, the second generation (gapmers) combined 2′-*O*-alkyl nucleotides[7–9] and phosphorothioate/phosphodiester units. This generation seems to be providing promising ON constructs for further therapeutic development. So far, hundreds of synthetic alternatives have been introduced, and their properties assessed.[5,10] Currently, there are numerous modifications available for *in vivo* experiments, including methylphosphonates,[11] boranophosphates[12] (recruiting RNase H activity[13]), cyclohexenyl oligonucleotides,[14] morpholino ONs,[15,16] *N3′→P5′* phosphoramidates,[17,18] LNA,[19–22] and PNA.[23] The recently published screening study on various siRNA oligonucleotides constructed with a number of currently existing chemical modifications formulated certain guidelines for efforts to enhance siRNA activities through chemical modifications, which further highlighted the role of the often subtle structural alterations.[24] In addition, the discovery of miRNAs[25] as therapeutic targets for antisense oligonucleotides revived chemists' interest in these compounds.[26] Undoubtedly, the complexity of problems associated with specifying suitable candidates for practical use of oligonucleotides as efficient therapeutics still warrants further research on novel modifications of the sugar–phosphate backbone to achieve optimal oligonucleotide properties.

We have devoted considerable attention to the nuclease-stable, phosphonate-based internucleotide linkages.[27–31] Recently, we reported a study on the conformation of a novel phosphonate *C3′-O-P-CH₂-O-C4′* internucleotide linkage isosteric to that of the natural phosphodiester *C3′-O-P-O-CH₂-C4′* bond. In contrast to the natural unit **2**, we found that the sugar moiety of the nucleoside phosphonate units[31] **1a** and **1b** occurred predominantly in the *C2′-endo* (~95%, *S*-type) and *C3′-endo* (~98%, *N*-type) conformations, respectively (Fig. 1).

This dramatic difference in the sugar ring conformation seems to be related to the *anomeric effect*[32] elicited by the presence of an exocyclic oxygen atom attached to the C4′ carbon. Considering these findings, we concluded that also 4′-alkoxy-2′-deoxynucleosides **3a** and **3b** could exhibit a similar conformational behaviour,[33–35] and that, in all likelihood, the incorporation of **3a** with preferential *C3′-endo* conformation[35] into the phosphodiester oligodeoxynucleotides would give rise to new interesting chimeras that hybridise well to a complementary RNA. We started with thymine as the nucleobase because of its natural relation to the 2′-deoxysugar moiety, but uracil would have also been justified with regard to the prevailing C3′-*endo* (RNA-type) conformation of the 4′-alkoxy-2′-deoxyribose sugar moiety.

Thus, in this paper, we describe two types of 4′-alkoxy oligothymidylates and compare their hybridisation properties towards dA_{15} and rA_{15} with those of the natural oligothymidylate and 2′-*O*-methyl-oligoribothymidylate.

[a]*Institute of Organic Chemistry and Biochemistry, Academy of Sciences of the Czech Republic, v. v. i., Flemingovo 2, 166 10 Prague 6, Czech Republic. E-mail: rosenberg@uochb.cas.cz*
[b]*Division of Biomolecular Physics, Institute of Physics, Faculty of Mathematics and Physics, Charles University, Ke Karlovu 5, 12116 Prague 2, Czech Republic*

† Electronic supplementary information (ESI) available. See DOI: 10.1039/c1ob06148h

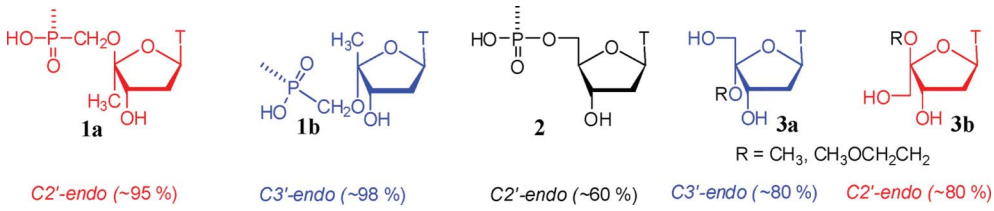

Fig. 1 Sugar pucker of the 4′-phosphonoalkoxy and 4′-alkoxynucleoside units.

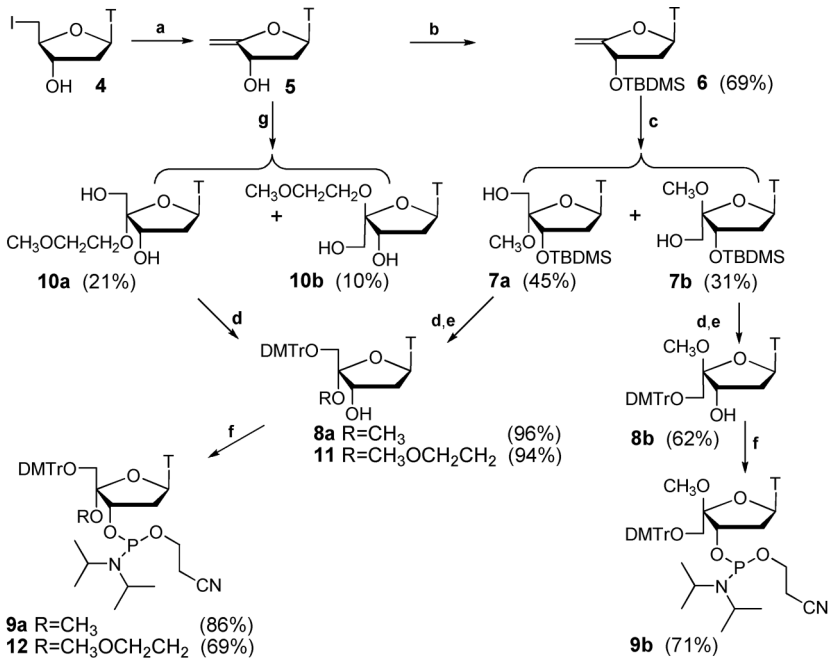

a 0.5 M-CH_3ONa-methanol, reflux for 8 h; **b** TBDMSCl, imidazole, pyridine, 8 h at r. t.; **c** methanol, 70% MCPBA, 5 h at r. t., a silica gel separation of epimers; **d** DMTrCl, pyridine; **e** TBAF, THF, 16 h at r. t.; **f** 2-cyanoethoxy-N,N-diisopropylaminochlorophosphine, DIPEA, THF, 40-60 min at r. t.; **g** 2-methoxyethanol, MCPBA, 4 h at r. t., a silica gel separation of epimers

Scheme 1 Synthesis of protected 4′-alkoxypentofuranosylthymine-3′-cyanophosphoramidites **9a,9b**, and **12**.

Results and discussion

Chemistry

Synthesis of monomers for oligonucleotide synthesis. *4′-Epimeric 4′-methoxypentofuranosylthymine-3′-phosphoramidites* (**9a** and **9b** in Scheme 1). The 5′-iodo derivative **4**[36] prepared from 2′-deoxythymidine and a triphenylphosphine–iodine complex was dehydrohalogenated with sodium methoxide, providing a good yield of the 4′,5′-didehydro compound **5**.[37] Its treatment with *tert*-butyldimethylsilyl chloride afforded the silyl derivative **6**.[38] The electrophilic addition of methanol in the presence of *m*-chloroperbenzoic acid provided the desired 4′-methoxy epimers, **7a** and **7b**, which were easily separable on silica gel in good yields of 45% and 31%, respectively. The assignment of C4′ configuration in **7a** and **7b** and their desilylated derivatives, **3a** and **3b** (see below and in the ESI† p. S8–S12), was made by NMR spectroscopy. This was in agreement with previously published data.[39] Both epimers, **7a** (α-L-*threo*) and **7b** (β-D-*erythro*), were protected by a dimethoxytrityl group in the 5′ position, and the appropriate 5′-dimethoxytrityl derivatives were treated, after extraction into DCM, with TBAF in THF to afford compounds **8a** and **8b**, respectively. Subsequent phosphitylation of the free 3′-hydroxyl groups with 2-cyanoethoxy-*N*,*N*-diisopropylaminochlorophosphine afforded the phosphoramidites **9a** and **9b** as the units for oligonucleotide assembly.

4′-(2-Methoxyethoxy)thymidine-3′-phosphoramidite **12** (Scheme 1). The 4′,5′-didehydro compound **5** was treated with anhydrous 2-methoxyethanol and *m*-chloroperoxybenzoic acid to yield the epimeric 4′-(2-methoxythoxy) derivatives **10a** and **10b**, which were separated by silica gel chromatography. Only the former, resembling the structure of dT, was further derivatized. Dimethoxytritylation afforded derivative **11** which was phosphitylated with 2-cyanoethoxy-*N*,*N*-diisopropylaminochlorophosphine to yield the desired monomer **12**.

Conformational analysis of 4′-methoxynucleosides 3a and 3b. The key compounds that inspired this work, the nucleosides **3a** and **3b**, have been previously reported,[37,39] and the configuration of these 4′-epimers was assigned by Chattopadhyaya.[39] Because we worked with the 3′-*O*-silylated starting compound **6** (not 3′-OH or 3′-OAc, as in references[37,39]), to prepare the respective 4′ epimers in good yields we needed assurance of the reaction outcome, isomeric purity, and unambiguous configuration assignments. In addition, we wanted to learn more about the conformational preferences of these individual isomers.

The configuration at carbon C4′ and preferred orientation of thymine in compounds **3a** and **3b** was determined from the observed NOE contacts in the 2D-H,H-ROESY spectra in DMSO (Fig. S1†). The absence of hydrogen on the C4′ reduces the number of proton vicinal couplings and limits the common NMR conformation analysis using the PSEUROT[40,41] program. Therefore we used an approximate method for the estimation of the population of "south"-type conformers (usually C2′-*endo*) based on eqn ([1]), as described for deoxyribonucleosides by Rinkel and Altona.[42]

$$(\%)\ \text{south C2′-}endo\ \text{conformer} = [31.5 - J(1',2'') - J(2',2'') - J(2'',3')]/10.9] \times 100 \quad (1)$$

The observed *J*-values in **3a** (Fig. S1†) then lead to a high preference for the "north"-type C3′-*endo* conformation (~84%). On the other hand, the observed *J*-values in **3b** (Fig. S1†) indicate a high population of "south"-type C2′-*endo* conformers (~83%). To support the results obtained from ^{1}H NMR conformational analysis using eqn ([1]), we explored the conformational behaviour of compounds **3a** and **3b** by molecular modelling. We used the well-known concept of pseudorotation[43] for the sugar ring conformation of nucleosides and calculated the endocyclic torsion angles. The results of this analysis showed a 98% preference for an N-pucker in **3a** and an 84% population of an S-pucker in **3b** (Table S2†). This is in good agreement with experimental NMR data and confirms our discussions on the MDS results and overall structural relationships.

Hybridisation study (Table 1)

All oligothymidylates were synthesized by a phosphoramidite method on solid phase according to the standard protocol. Measurements of the thermal characteristics of the oligonucleotide complexes were performed at 260 and 295 nm on a CARY 100 Bio UV Spectrophotometer equipped with a Peltier temperature controller and thermal analysis software. In all cases, we observed a single transition profile. T_m values were determined from the first derivative plots (dA_{260}/dT *versus* temperature) as the temperatures corresponding to the local maxima of dA_{260}/dT (see Table 1; for profiles see ESI† p. S22–S36).

Characterization of the type of the complexes was performed by a native PAGE at 15 °C in the presence of sodium or magnesium ions (see ESI† p. S39–S41). PAGE revealed formation of triplexes of dT_{15} (entry 1) and $(_{4'\text{-MeOEtO}}T)_{14}T$ (entry 4) with rA_{15}, and also of $(_{4'\text{-MeO}}T)_{14}T$ (entry 5) with dA_{15} only in the presence of magnesium ions, which are known to promote the triple helical structure.[44] Interestingly, the $(T_{2'\text{-OMe}})_{14}T$ oligomer (entry 2) used as a reference compound formed under these conditions the duplex as did also the remaining studied oligomers. Surprisingly, the complex $(_{4'\text{-MeOEtO}}T)_{14}T$-$dA_{15}$-$Mg^{2+}$ (Entry 4) exhibiting a high T_m value showed only a weak band on the PAGE corresponding, by the mobility shift, to the triplex (see ESI†, p. 40, Fig. S4, panel C, lane 4). This result was reproducible, and we do not have any plausible explanation for this phenomenon.

Since in several cases the complexes were not detected on the PAGE, we measured their thermal characteristics at 295 nm that should distinguish between the duplex and triplex structures.[45] Duplexes do not typically exhibit absorbance changes, whereas triplexes produce a negative melting curve (decreasing profile). In contrast to the PAGE we found in most cases negative profiles of melting curves suggesting the presence of a triplex structure (for the A_{295}-temperature plots see ESI† p. S39–S41). These results, quite different from those obtained by PAGE are difficult to explain. One can conclude that the measurement at 295 nm could be more sensitive to the presence of a triplex structure even at its very low equilibrium concentration. Therefore, in the following text, the terms duplex and triplex will refer to results obtained from PAGE.

To gain further insight into the structure of possible complexes formed, we measured the thermal difference spectra (TDS) obtained by the subtraction of the complexes' UV spectra measured above and below their T_m (60 and 15 °C, respectively). Normalisation of the TDS provided two types of patterns (see ESI† p. S37–S38). The first type is common for both dA_{15} and rA_{15} in the presence of Mg^{2+} ions (Mg-type), and the second type is common for dA_{15} and rA_{15} in the presence of Na^+ ions (Na-type). In contrast to the Mg-type with one negative local minimum, the Na-type exhibited two negative local minima. The shapes of the Na-type individual complexes were very complicated to interpret and did not seem to correspond to any typical pattern reported. In the light of these findings, we have evaluated the complexes based on the deconvolution of Raman or UV spectra of their complementary strand mixtures using the factor analysis.[46] This powerful method provides information on the number of statistically significant complexes, the equilibrium concentration of all components in a mixture (*i.e.*, duplex, triplex, and single strands), and enables the calculation of thermodynamic parameters. However, these results will be published elsewhere.

As obvious from Table 1, the complexes of $(_{4'\text{-MeOEtO}}T)_{14}T$ and $(_{4'\text{-MeO}}T)_{14}T$ oligomers (entries 4, 5) exhibited significantly increased thermal stabilities in comparison to the natural dT_{15} and $(_{4'\text{-Me}}T)_{14}T$,[30] but very similar to that of $(T_{2'\text{-OMe}})_{14}T$ (entry 3) prepared as a reference compound.

To examine the mutual conformational compatibility of the $_{4'\text{-MeOEtO}}T$, $_{4'\text{-MeO}}T$, and $T_{2'\text{-OMe}}$ units, we verified the thermal stabilities of complexes of the mixed oligothymidylates, $(_{4'\text{-MeOEtO}}T\text{-}_{4'\text{-MeO}}T)_7T$, $(_{4'\text{-MeOEtO}}TT_{2'\text{-OMe}})_7T$, and $(_{4'\text{-MeO}}TT_{2'\text{-OMe}})_7T$ (entries 9–11), with both dA_{15} and rA_{15}. Compared to dT_{15}, all three types of oligomers exhibited a decreased affinity towards dA_{15}-Na^+, a retained or slightly higher affinity towards dA_{15}-Mg^{2+}, and an increased affinity towards rA_{15}-Na^+ and rA_{15}-Mg^{2+}. All three modifications clearly exerted a similar and beneficial effect on hybridisation, which obviously arose from specific structural factors (discussed below in the MD study).

In contrast to these findings, the oligothymidylates $(T\text{-}T_{2'\text{-OMe}})_7T$ and $(T\text{-}_{4'\text{-MeO}}T)_7T$ (entries 7, 8) composed of natural thymidine and modified units exhibited a strongly reduced affinity towards both dA_{15} and rA_{15} in the presence of Na^+ ions compared to dT_{15} (Table 1). Both these types of oligomers had reduced T_m values (below the T_m of the natural dT_{15}) when in duplexes with dA_{15}-Mg^{2+}, but they retained their affinity towards rA_{15}-Mg^{2+}, similar to dT_{15}. This behaviour could be seen not only in the light of a different population of the individual sugar conformers in the T unit (~60% C2′-*endo*) on one hand and in $_{4'\text{-MeO}}T$ (~80% C3′-*endo*) or $_{2'\text{-MeO}}T$ units (~80% C3′-*endo*)[47] on the other, but also in the different dynamics of the individual conformational changes.

A disturbance of the binding of Na^+ or Mg^{2+} ions due to a lack of structural and conformational uniformity in the chain is

Table 1 Hybridisation properties of modified oligothymidylates with dA_{15} and rA_{15}

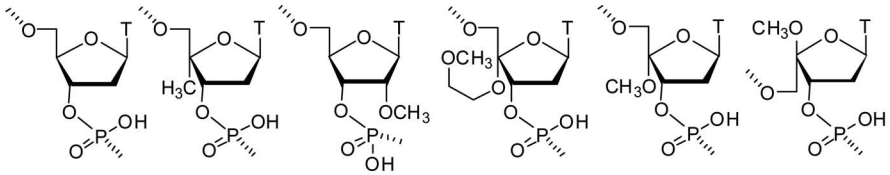

Entry	Modified dT_{15}	Melting point T_m [°C] [a] Complex type [b]			
		dA_{15}		rA_{15}	
		Na^+	Mg^{2+}	Na^+	Mg^{2+}
1	dT_{15}	**38** **duplex**	**48** **duplex**	**36** *no* [c]	**36** **triplex**
2	$(_{4'\text{-Me}}T)_{14}T$ [e]	<10 *no*	34 **duplex**	*nd* [d]	34 *no*
3	$(T_{2'\text{-OMe}})_{14}T$	35 *no*	54 **duplex**	48 **duplex**	55 **duplex**
4	$(_{4'\text{-MeOEtO}}T)_{14}T$	20 *no*	49 *no*	48 **duplex**	57 **triplex**
5	$(_{4'\text{-MeO}}T)_{14}T$	39 *no*	55 **triplex**	51 **duplex**	55 **duplex**
6	$(^{4'\text{-MeO}}T)_{14}T$	<10 *nd*	<10 *nd*	<10 *nd*	<10 *nd*
7	$(T\text{-}T_{2'\text{-OMe}})_7T$	19 *no*	35 *no*	33 *no*	38 **duplex**
8	$(T\text{-}_{4'\text{-MeO}}T)_7T$	19 *no*	37 **duplex**	<10 *no*	37 **duplex**
9	$(_{4'\text{-MeOEtO}}T\text{-}_{4'\text{-MeO}}T)_7T$	26 *nd*	53 *nd*	48 *nd*	57 *nd*
10	$(_{4'\text{-MeOEtO}}T\text{-}T_{2'\text{-OMe}})_7T$	22 *nd*	45 *nd*	41 *nd*	51 *nd*
11	$(_{4'\text{-MeO}}T\text{-}T_{2'\text{-OMe}})_7T$	28 *nd*	50 *nd*	41 *nd*	52 *nd*

[a] A 1:1 mixture of modified T_{15} with dA_{15} or rA_{15} at 4μM total strand concentrations were measured in 50 mM TRIS/HCl (pH 7.2, 1 mM EDTA with 10 mM Mg^{2+} or 100 mM Na^+); [b] duplex or triplex structures determined from the native PAGE at 15 °C (for conditions see ESI† p. S37-S41); [c] *no* … not observed; [d] *nd* … not determined; [e] reference 30

also likely to contribute to the destabilisation of these complexes. Concerning the role of the monovalent and divalent cations used in the present study in thermal stabilities, there was a significant difference in the T_m of $(_{4'\text{-MeO}}T)_{14}T$ and $(_{4'\text{-MeOEtO}}T)_{14}T$ complexed to dA_{15} in the presence of Na^+ ions. Compared to $(_{4'\text{-MeO}}T)_{14}T$, with a T_m value identical to that of natural dT_{15}, the $(_{4'\text{-MeOEtO}}T)_{14}T$ had a significantly lower T_m (~10 °C). A similar behaviour was observed when the mixed oligomers $(_{4'\text{-MeOEtO}}T\text{-}_{4'\text{-MeO}}T)_7T$, $(_{4'\text{-MeOEtO}}T\text{-}T_{2'\text{-OMe}})_7T$, and $(_{4'\text{-MeO}}T\text{-}T_{2'\text{-MeO}})_7T$ were examined in a complex with dA_{15} and Na^+ ions, with T_m values far below that of dT_{15} and the uniformly modified $(T_{2'\text{-OMe}})_{14}T$ and $(_{4'\text{-MeO}}T)_{14}T$. The reasons for these observations are suggested below in the section devoted to MDS.

We also prepared the oligothymidylate $(^{4'\text{-MeO}}T)_{14}T$ (entry 6) analogue, which also contained the C4′-methoxy units but epimeric to those in $(_{4'\text{-MeO}}T)_{14}T$ (entry 5). As we expected, this oligomer did not hybridise with any of the respective counterparts (dA_{15} or rA_{15}) due to the backbone with a different organisation.

MD studies

In contrast to the natural dT_{15}, which hybridises more efficiently with dA_{15} than with rA_{15}, the oligomers $(_{4'\text{-MeO}}T)_{14}T$, $(_{4'\text{-MeOEtO}}T)_{14}T$, and $(T_{2'\text{-OMe}})_{14}T$ hybridised more tightly with rA_{15}. This correlates with the *ab initio* calculations and NMR findings showing the preferential C3′-*endo* conformation of the sugar moieties in the corresponding nucleosides.

To gain further knowledge on how the measured thermal stabilities (T_m) are related to the structures of the novel oligomers, we performed molecular dynamics simulations (MDS) with model oligonucleotide triple helical structures carrying chemical modifications on their either C4′ or C2′ atoms: $T(_{4'\text{-MeO}}T)_8T{\cdot}rA_{10}{*}T(_{4'\text{-MeO}}T)_8T$, $T(_{4'\text{-MeOEtO}}T)_8T{\cdot}rA_{10}{*}T(_{4'\text{-MeOEtO}}T)_8T$, and $T(T_{2'\text{-OMe}})_8T{\cdot}rA_{10}{*}T(T_{2'\text{-OMe}})_8T$ (· denotes Watson–Crick base pairing, and * indicates Hoogsteen base pairing). Method details are provided in the ESI.†

Intra-strand effects – The C2′-OCH_3 moieties in the $T_{2'\text{-OMe}}$-modified chain were buried within the nucleic acid grooves (Fig. S5–S6†), and the CH_3 groups interacted tightly with the C5′ atoms of the neighbour nucleotide residues through hydrophobic effects. Moreover, the CH_3 groups partially shielded the mutual repulsion between the polarised O2′, O2, and O4′ atoms. Therefore, the intra-strand hydrophobic and electrostatic complementarity effects could boost-stimulate helical preorganization and provide additional stabilisation. In contrast, the surprisingly low melting temperature (20 °C) observed for the $(_{4'\text{-MeOEtO}}T)_{14}T$-$dA_{15}$-$Na^+$ complex (Table 1, entry 4) could have been caused by a crowding together of the central hydrophobic portions of the C4′-$OCH_2CH_2OCH_3$ moieties in the $_{4'\text{-MeOEtO}}T$ chain, affecting the ability of $(_{4'\text{-MeOEtO}}T)_{14}T$ to organise into a helix-like structure.

Direct inter-strand effects – In the triple helical structures, the $(_{4'\text{-MeO}}T)_8T$ and $(_{4'\text{-MeOEtO}}T)_8T$ Hoogsteen strands (light blue in Fig. 2, 3, S7–S10†) divided the major groove, thus creating the *minor-major* and *major-major* grooves. The former was very narrow, and the alkoxy groups in $_{4'\text{-MeO}}T$ and $_{4'\text{-MeOEtO}}T$ units were oriented towards the phosphate groups of the central dA_{15}/rA_{15}. Nevertheless, no apparent steric conflict was found, even in the case of the relatively bulky C4′-$OCH_2CH_2OCH_3$ moiety in the $_{4'\text{-MeOEtO}}T$ unit bridging the *minor-major* groove. On the other hand, there were no suitable hydrogen-bond donors in the dA_{15}/rA_{15} chains that could provide direct inter-strand stabilisation through interactions with the oxygen atoms of the alkoxy groups in the $_{4'\text{-MeO}}T$-, $_{4'\text{-MeOEtO}}T$-, and $T_{2'\text{-OMe}}$-modified strands.

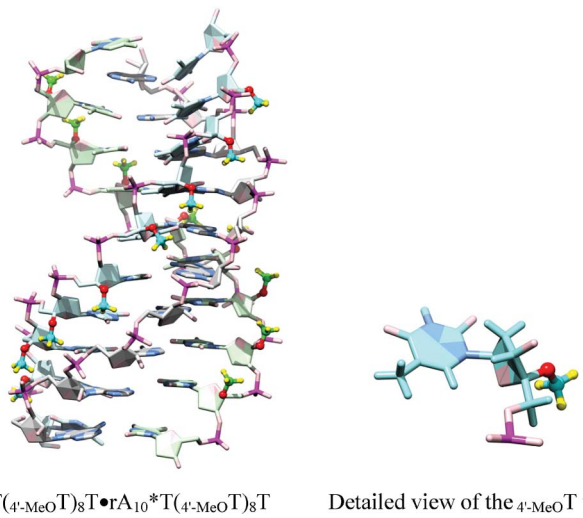

$T(_{4'\text{-MeO}}T)_8T{\bullet}rA_{10}{*}T(_{4'\text{-MeO}}T)_8T$ Detailed view of the $_{4'\text{-MeO}}T$ unit

Fig. 2 Triple helical structure of $T(_{4'\text{-MeO}}T)_8T{\cdot}rA_{10}{*}T(_{4'\text{-MeO}}T)_8T$ used as a model in the MD simulations. Enlarged versions of these pictures (either with or without hydrogen atoms) are provided in the ESI† (Fig. S7, S8), including those produced for the reference triple helical structure $T(T_{2'\text{-OMe}})_8T{\cdot}rA_{10}{*}T(T_{2'\text{-OMe}})_8T$ (Fig. S5–S6).

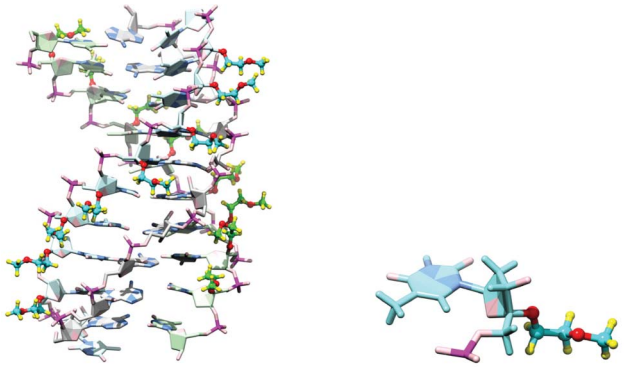

$T(_{4'\text{-MeOEtO}}T)_8T{\bullet}rA_{10}{*}T(_{4'\text{-MeOEtO}}T)_8T$ Detailed view of the $_{4'\text{-MeOEtO}}T$ unit

Fig. 3 Triple helical structure of $T(_{4'\text{-MeOEtO}}T)_8T{\cdot}rA_{10}{*}T(_{4'\text{-MeOEtO}}T)_8T$ used as a model in the MD simulations. Enlarged versions of these pictures (either with or without hydrogen atoms) are provided in the ESI† (Fig. S9, S10), including those produced for the reference triple helical structure $T(T_{2'\text{-OMe}})_8T{\cdot}rA_{10}{*}T(T_{2'\text{-OMe}})_8T$ (Fig. S5–S6).

Solvent mediated inter-strand effects – Nevertheless, additional stabilisation could have been provided by water molecules and cations. The thermal stabilities of the $(_{4'\text{-MeO}}T)_{14}T$ complexes with dA_{15}/rA_{15}, expressed as T_m values, were slightly higher than that of $(T_{2'\text{-OMe}})_{14}T$. Interestingly, these differences were more pronounced with Na^+ rather than Mg^{2+} ions (Table 1). Na^+ ions were found to reside in the proximity of C4′-OCH_3 groups if partial atomic charges on oxygen atoms were calculated by either the CHARMM force field or the *ab initio* Mulliken equations instead of the original AMBER/RESP method. In this case, the oxygen atoms of the 4′-OCH_3 and O3′-phosphoester groups (originating from the same chain) were directly involved in Na^+-ion binding (Fig. S14†). Consequently, the Na^+ ions residing in the nucleic-acid grooves diminished the interstrand repulsion between the nucleic acids chains. The Na^+ ions are only weakly bound to the ligands and interchange many binding sites within the MD runs. In contrast, the Mg^{2+} ions are usually firmly anchored towards the ligands, with residence times that typically exceeded the duration of the MD runs. Surprisingly, the Mg^{2+} ions placed in the Na^+ binding sites of the nearby of C4′-OCH_3 groups escaped quickly towards the non-bridging oxygen atoms of the phosphate groups (O1P) located in the same oligonucleotide chain. Aside from the strong coulombic attraction of the highly charged Mg^{2+}-O1P atoms, the substantially smaller van der Waals radius of the Mg^{2+} ions (compared to Na^+) played a role in locking the C4′-alkoxy sugars in a labile intermediate conformer position between the C2′- and C3′-*endo* energy minima. Such a position did not last long, and the sugars typically underwent a conformational transition accompanied by the Mg^{2+} ions escaping towards the O1P atoms within tens or hundreds of picoseconds.

Interestingly, the Hoogsteen $(_{4'\text{-MeOEtO}}T)_{14}T$ chains carrying the C4′-$OCH_2CH_2OCH_3$ groups could share the Mg^{2+} ions in triple helical structures with phosphate groups from the central adenosine strand (Fig. 4, S13†). This could partly explain the highest measured melting temperatures (57 °C) determined for the $[(_{4'\text{-MeOEtO}}T)_{14}T]$-$rA_{15}$-$Mg^{2+}$ and $[(_{4'\text{-MeOEtO}}T\text{-}_{4'\text{-MeO}}T)_7T]$-$rA_{15}$-$Mg^{2+}$ systems (Table 1, entries 4 and 9). Therefore, the Mg^{2+} ions were placed in the proximity of non-bridging oxygen atoms from the phosphate groups of the rA_{15} strand, as is found in many X-ray structures. The C4′-$OCH_2CH_2OCH_3$ groups were also adjusted to interact with the Mg^{2+} ions (Fig. S11–S12†). Two contacts between the Mg^{2+} ion and the C4′-$OCH_2CH_2OCH_3$ moiety involving both or only the terminal oxygen atoms were tested. The former configuration (Mg^{2+}- C4′$\underline{O}CH_2CH_2\underline{O}CH_3$) resulted in more stable contacts, so that the Hoogsteen $(_{4'\text{-MeOEtO}}T)_{14}T$ strand and rA_{15} were tightly attached together (Fig. 4, S13†). However, the resulting triple helical structure was slightly disturbed in the centre. On the other hand, the latter configuration (Mg^{2+}- C4′$OCH_2CH_2\underline{O}CH_3$) resulted in less stable contacts, but the resulting triple helical structure was more similar to the natural triplex.

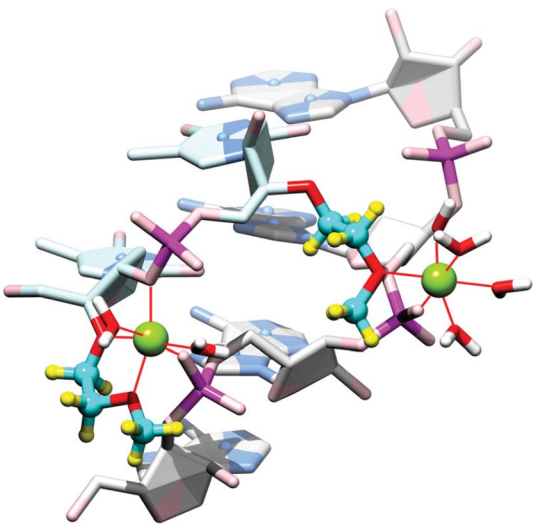

Fig. 4 Two modes of contact between Mg^{2+} ions and C4′-OCH_2CH_2-OCH_3 groups in the $(_{4'\text{-MeOEtO}}T)28$, $(_{4'\text{-MeOEtO}}T)29$ and rA6-rA9 portions of the Hoogsteen strand of the $[T(_{4'\text{-MeOEtO}}T)_8T]^{W\text{-}C}\cdot rA_{10}{*}[T(_{4'\text{-MeOEtO}}T)_8T]^{Hgstn}$ triplex, where rA_{10} consists of residues 1–10, Watson–Crick pyrimidine strand – residues 11–20, and Hoogsteen strand – residues 21–30. The enlarged version is available in the ESI† (Fig. S13), where binding of Mg^{2+} ions in the context of the whole triple helical structure can be found as well (Fig. S11, S12†).

Conclusion

In summary, we have presented a new and promising structural alternative to the existing analogues of the natural phosphodiester oligonucleotides. Modifications involving the presence of either a 4′-methoxy or 4′-(2-methoxyethoxy) group in oligothymidylates, represented by the $(_{4'\text{-MeO}}T)_{14}T$ and $(_{4'\text{-MeOEtO}}T)_{14}T$ oligonucleotides, were found to display markedly better hybridisation properties with both the dA_{15} and rA_{15} counterparts compared to unmodified dT_{15}. The novel oligomers containing the $_{4'\text{-MeOEtO}}T$ and $_{4'\text{-MeO}}T$ units are DNA constructs that mimicked the RNA behaviour comparably as phosphoramidate oligodeoxynucleotides.[48] The observed T_m enhancement was of similar magnitude to that of the respective 2′-*O*-methyl group-containing $(T_{2'\text{-OMe}})_{14}T$ used as a reference oligonucleotide, thus confirming the original assumption that these two types of modifications sharing the presence of an *N*-type sugar pucker in the parent nucleoside could provide oligonucleotides with similar hybridisation properties. We are aware of the importance of creating the mixed purine–pyrimidine 4′-alkoxyoligonucleotides (*i.e.*, containing all of the U, C, A, and G nucleobases) for their direct use in biological experiments. Therefore, we are currently working on a straightforward synthesis of 4′-alkoxy-2′deoxynucleosides in the purine series to make these compounds practically available on a preparative scale. We believe that the 4′-alkoxy-2′-deoxynucleosides will be interesting building units for assembly of the phosphodiester 4′-alkoxyoligodeoxynucleotides as new interesting RNA chimeras.[49]

Experimental

Synthesis of monomers

Preparation of the final nucleoside phosphoramidites for oligonucleotide assembly and characterisation of compounds is described in detail in the ESI.†

Synthesis of oligonucleotides

All oligonucleotides (Table 1) were synthesised from the appropriate monomers on a ~0.5 μmol scale by a standard phosphoramidite method using the LCAA CPG with attached 5′-*O*-dimethoxytritylthymidine-3′-*O*-hemisuccinate as the first nucleoside. Deprotection and release of each oligonucleotide from CPG was achieved with gaseous ammonia (0.7 MPa) at r.t. for 8 h. Oligonucleotides were purified on Luna C18 columns (5 μm, 10 × 250 mm) at a flow rate 3 ml min^{-1} using a linear gradient of acetonitrile (0→50%, 40 min) in 0.1 M TEAA (pH 7.2 at r.t.) and finally freeze-dried. All prepared oligonucleotides were characterised by MALDI TOF (Table S1†).

Stability of the modified oligothymidylates towards nucleases

The stability of the homooligomers $(_{4'\text{-MeO}}T)_{14}T$ and $(_{4'\text{-MeOEtO}}T)_{14}T$ was verified under conditions described earlier.[50] Complete stability in the L1210 cell-free extract and in the presence of endonuclease P1 (EC 3.1.3.16) was observed. Experiments carried out under conditions in which halftime cleavage of the natural dT_{15} was less than 1 min showed that no cleavage of the modified oligomers occurred within 2 h (determined by HPLC). However, no resistance was found against snake venom exonuclease (EC 3.1.30.1).

Hybridisation study (Table 1)

Thermal experiments with oligonucleotide complexes were performed at 260 and 295 nm on a CARY 100 Bio UV Spectrophotometer (Varian Inc.) equipped with a Peltier temperature controller and thermal analysis software. An equimolar mixture of modified T_{15} and natural dA_{15} (or rA_{15}) strands was prepared to give a final concentration of 4 μM in 50 mM Tris-HCl (pH 7.2) and 1 mM EDTA containing either 100 mM Na^+ or 10 mM

Mg^{2+} ions. A heating–cooling cycle over a range of 18–90 °C with a gradient of 0.5 °C min^{-1} was applied. T_m value of each complex was determined from the first derivative plots (dA_{260}/dT *versus* temperature) as the temperature at a local maximum of dA_{260}/dT. For thermal stability curves at 260 and 295 nm and 1st derivation dA_{260}/dT *versus* T plots see the ESI† (p. S32–S36).

Determination of the type of complex by PAGE

Modified oligonucleotides (mT_{15}) were mixed with (^{32}P) 5′-end labelled dA_{15} or rA_{15} in 10 mM Tris (pH 7.4) and 150 mM NaCl (or 10 mM $MgCl_2$) at 1 : 1 molar ratios to obtain final concentrations of 100 nM. Individual annealings were performed by heating the mixtures to 80 °C and cooling them slowly to room temperature. The samples were then mixed with 10 mM Tris (pH 7.4) and 20% glycerol in a 1 : 1 ratio and loaded onto 20% native polyacrylamide gels. Electrophoresis was run in 1xTBE (or 1xTB with 10 mM $MgCl_2$) at 12.5 V cm^{-1} for 10 h at 15 °C. The gels were dried and visualised by autoradiography (Fig. S4,† p. S39–S40).

Acknowledgements

Support from the grant 202/09/0193 (Czech Science Foundation) and the Research Centres KAN200520801 (Acad. Sci. CR) and LC060061 (Ministry of Education, CR), under the Institute research project Z40550506, are gratefully acknowledged, in addition to support by project No. MSM 0021620835 (Ministry of Education, CR). The authors thank the staff of the Mass Spectrometry Group of the IOCB AS, v.v.i. (Dr Josef Cvačka, Head) for the HR-MS spectra.

References

1 P. C. Zamecnik and M. L. Stephenson, *Proc. Natl. Acad. Sci. U. S. A.*, 1978, **75**, 280–284.
2 E. Uhlmann and A. Peyman, *Chem. Rev.*, 1990, **90**, 543–584.
3 S. T. Crooke, *Annu. Rev. Med.*, 2004, **55**, 61–95.
4 I. Lebedeva and C. A. Stein, *Annu. Rev. Pharmacol. Toxicol.*, 2001, **41**, 403–419.
5 J. Kurreck, in *TherapeuticOligonucleotides*, ed. J. Kurreck, RSC Publishing, Cambridge (UK), 2008, pp. 1–22.
6 F. Eckstein, *Antisense Nucleic Acid Drug Dev.*, 2000, **10**, 117–121.
7 A. M. Iribarren, B. S. Sproat, P. Neuner, I. Sulston, U. Ryder and A. I. Lamond, *Proc. Natl. Acad. Sci. U. S. A.*, 1990, **87**, 7747–7751.
8 C. Boiziau, B. Larrouy, B. S. Sproat and J. J. Toulmé, *Nucleic Acids Res.*, 1995, **23**, 64–71.
9 M. Manoharan, *Biochim. Biophys. Acta*, 1999, **1489**, 117–130.
10 S. M. Freier and K. H. Altmann, *Nucleic Acids Res.*, 1997, **25**, 4429–4443.
11 M. A. Reynolds, R. I. Hogrefe, J. A. Jaeger, D. A. Schwartz, T. A. Riley, W. B. Marvin, W. J. Daily, M. M. Vaghefi, T. A. Beck, S. K. Knowles, R. E. Klem and L. J. Arnold, Jr., *Nucleic Acids Res.*, 1996, **24**, 4584–4591.
12 D. Sergueev, A. Hasan, M. Ramaswamy, B. R. Shaw and P. M. Gross, *Nucleosides Nucleotides Nucl. Acids*, 1997, **16**, 1533–1538.
13 X. Wang, M. Dobrikov, D. Sergueev and B. R. Shaw, *Nucleosides Nucleotides Nucl. Acids*, 2003, **22**, 1151–1153.
14 K. Nauwelaerts, E. Lescrinier, G. Sclep and P. Herdewijn, *Nucleic Acids Res.*, 2005, **33**, 2452–2463.
15 J. Summerton and D. Weller, *Antisense Nucleic Acid Drug Dev.*, 1997, **7**, 187–195.
16 J. Heasman, *Dev. Biol.*, 2002, **243**, 209–214.
17 M. Faria, D. G. Spiller, C. Dubertret, J. S. Nelson, M. R. H. White, D. Scherman, C. Hélène and C. Giovannangeli, *Nat. Biotechnol.*, 2001, **19**, 40–44.
18 B. Shea-Herbert, K. Pongracz, J. W. Shay and S. M. Gryaznov, *Oncogene*, 2002, **21**, 638–642.
19 S. K. Singh, P. Nielsen, A. A. Koshkin and J. Wengel, *Chem. Commun.*, 1998, 455–456.
20 M. Petersen and J. Wengel, *Trends Biotechnol.*, 2003, **21**, 74–81.
21 S. Obika, D. Nanbu, Y. Hari, K. Morio, Y. In, T. Ishida and T. Imanishi, *Tetrahedron Lett.*, 1997, **38**, 8735–8738.
22 D. Honcharenko, J. Barman, O. P. Varghese and J. Chattopadhyaya, *Biochemistry*, 2007, **46**, 5635–5646.
23 M. Egholm, O. Buchardt, L. Christensen, C. Behrens, S. M. Freier, D. Driver, R. H. Berg, S. K. Kim, B. Nordén and P. E. Nielsen, *Nature*, 1993, **365**, 566–568.
24 J. B. Bramsen, M. B. Laursen, A. F. Nielsen, T. B. Hansen, C. Bus, N. Langkjær, B. R. Babu, T. Højland, M. Abramov, A. Van Aerschot, D. Odadzic, R. Smicius, J. Haas, C. Andree, J. Barman, M. Wenska, P. Srivastava, C. Zhou, D. Honcharenko, S. Hess, E. Müller, G. V. Bobkov, S. N. Mikhailov, E. Fava, T. F. Meyer, J. Chattopadhyaya, M. Zerial, J. W. Engels, P. Herdewijn, J. Wengel and J. Kjems, *Nucleic Acids Res.*, 2009, **37**, 2867–2881.
25 R. C. Lee, R. L. Feinbaum and V. Ambros, *Cell*, 1993, **75**, 843–854.
26 C. Davis, B. Lollo, S. Freier and C. Esau, *Nucleic Acids Res.*, 2006, **34**, 2294–2304.
27 I. Rosenberg, in *Frontiers in Nucleosides and Nucleic Acids*; ed. R. F. Schinazi and D. C. Liotta, IHL Press, Tucker, GA, 2004, pp. 519–548.
28 V. Vaněk, M. Buděšínský, M. Rinnová and I. Rosenberg, *Tetrahedron*, 2009, **65**, 862–876.
29 D. Rejman, P. Kočalka, R. Pohl, Z. Točík and I. Rosenberg, *Collect. Czech. Chem. Commun.*, 2009, **74**, 935–955.
30 Z. Točík, I. Barvík Jr., M. Buděšínský and I. Rosenberg, *Biopolymers*, 2006, **83**, 400–413.
31 Z. Točík, I. Barvík Jr., M. Buděšínský and I. Rosenberg, *Biopolymers*, 2009, **91**, 514–529.
32 C. Thibodeau, P. Acharya and J. Chattopadhyaya, *Stereoelectronic effects in nucleosides and nucleotides and their structural implications*, Uppsala University Press, ISBN 91-506-1351-0, 2nd Ed., Uppsala, 2003.
33 J. P. H. Verheyden and J. G. Moffat, *J. Am. Chem. Soc.*, 1975, **97**, 4386–4395.
34 H. Maag, R. M. Rydzewski, M. J. McRoberts, D. Crawford-Ruth, J. P. H. Verheyden and E. J. Prisbe, *J. Med. Chem.*, 1992, **35**, 1440–1451.
35 W. Tong, P. Agback and J. Chattopadhyaya, *Acta Chem. Scand.*, 1993, **47**, 145–156.
36 P. J. Garegg and B. Samuelsson, *J. Chem. Soc., Perkin Trans. 1*, 1980, 2866–2869.
37 H. Maag, R. M. Rydzewski, M. J. McRoberts, D. Crawford-Ruth, J. P. H. Verheyden and E. J. Prisbe, *J. Med. Chem.*, 1992, **35**, 1440–1451.
38 Z. Točík, I. Dvořáková, R. Liboska, M. Buděšínský, M. Masojídková and I. Rosenberg, *Tetrahedron*, 2007, **63**, 4516–4534.
39 W. Tong, P. Agback and J. Chattopadhyaya, *Acta Chem. Scand.*, 1993, **47**, 145–156.
40 J. van Wijk, C. A. G. Haasnoot, F. A. A. M. de Leeuw, B. D. Huckriede, A. Westra Hoekzema and C. Altona, *PSEUROT 6.2 1993*, PSEUROT 6.3 1999; Leiden Institute of Chemistry, Leiden University.
41 F. A. A. M. de Leeuw and C. Altona, *J. Comput. Chem.*, 1983, **4**, 428–437.
42 L. J. Rinkel and C. Altona, *J. Biomed. Struct. Dyn.*, 1987, **4**, 621–649 .
43 C. Altona and M. Sundaralingam, *J. Am. Chem. Soc.*, 1972, **94**, 8205–8212.
44 D. Coman and I. M. Russu, *Nucleic Acids Res.*, 2004, **32**, 878–883.
45 J.-L. Mergny, J. Li, L. Lacroix, S. Amrane and J. B. Chaires, *Nucleic Acids Res.*, 2005, **33**, e138.
46 J. Hanuš, I. Barvík, K. Ruszová-Chmelová, J. Štěpánek, P.-Y. Turpin, I. Rosenberg and M. Petrová-Endová, *Nucleic Acids Res.*, 2001, **29**, 5182–5194.
47 B. Bhat, E. E. Swayze, P. Wheeler, S. Dimock, M. Perbost and Y. S. Sanghvi, *J. Org. Chem.*, 1996, **61**, 8186–8199.
48 M. Egli and S. M. Gryaznov, *Cell. Mol. Life Sci.*, 2000, **57**, 1440–1456.
49 M. Koizumi, *Curr. Topics Med. Chem.*, 2007, **7**, 661–665.
50 D. Rejman, J. Snášel, R. Liboska, Z. Točík, O. Pačes, Š. Králíková, M. Rinnová, P. Koiš and I. Rosenberg, *Nucleosides Nucleotides Nucl. Acids*, 2001, **20**, 819–823.